C.M. Sonsino[1] and R. Pfohl[2]

MULTIAXIAL FATIGUE OF WELDED SHAFT-FLANGE CONNECTIONS OF STIRRERS UNDER RANDOM NON-PROPORTIONAL TORSION AND BENDING

Reference: Sonsino, C.M. and Pfohl, R., "Multiaxial Fatigue of Welded Shaft-Flange Connections of Stirrers under Random Non-Proportional Torsion and Bending", Third International Conference on Biaxial/Multiaxial Fatigue, April 3-6, 1989, Stuttgart, Fed. Rep. of Germany.

Abstract: Multiaxial fatigue failures of welded coupling flanges of stirrers in a fertilizer plant required an investigation of the reasons for the failures and to develop an improved design. Strain measurements carried out at the shaft showed that the stirrers experienced fluctuating torsional loads due to upward and downward driving from the gearbox and bending loads due to the viscous fluid stirred by impellers at the bottom of the shafts. The analysis of this variable amplitude loading resulted in two particular cumulative frequency distributions for torsion and bending which then had to be combined to a single equivalent loading spectrum and extrapolated to the estimated period of usage. When using this spectrum for the combined multiaxial loading of the shafts and an appropriate damage accumulation hypothesis, the failures of the welds could be explained and a redesign and optimization of the shaft-flange connections achieved.

Key words: Multiaxial fatigue, random loading, bending, torsion, welds, equivalent stress, fatigue life calculation, design

1 INTRODUCTION

Ten years ago several multiaxial random fatigue failures of welded coupling flanges of stirrers, Fig. 1, in a fertilizer plant occured after a relatively short service life of about six months. Thus Lurgi and LBF were involved as consultants in order to clarify the reasons for the failures and to develop an improved design with a required minimum fatigue life of ten years.

In the following it will be explained how the multiaxial random loads and the original design were evaluated in order to improve and optimize the shaft-flange connections and to avoid failures.

---

1) Fraunhofer-Institut für Betriebsfestigkeit (LBF), Darmstadt
2) Lurgi GmbH, Frankfurt, Fed. Rep. of Germany

2 EVALUATION OF ORIGINAL DESIGN AND LOAD ANALYSIS

2.1 Original Design

Fig. 2a shows the original design of the welded flange-shaft connection, which encountered no operational problems on small scale stirrers. The design of the small scale stirrers based on simple calculations and extensive experiences of the manufacturer. However, in the big scale version early fatigue cracks started from the welds which were finished by turning and led to total failures after approximately six months of operation corresponding to about $7 \cdot 10^6$ cycles. This number of cycles indicated either an endurance limit or a random fatigue problem.

As the welds were obviously in a region of high stress concentration because of the relatively sharp radius between flange and shaft and the sharp diversion of the loads from one shaft into the other one by the eight bolts around the flanges, the manufacturer accepted the advice to remove the weld into an area of lower stress concentration, Fig. 2b. But this design seemed to be critical, too, because of the sharp stress raisers in the inner diameter of the weld. In order to persuade the manufacturer load measurements were recommended.

2.2 Load analysis

The loadings were measured with strain gauges applied at the shaft of the stirrers [1]. Fig. 3 shows the load-time histories of the torsional and bending loadings.

The comparison of the load-time histories shows that the torsional loading has a higher frequency than the bending loading and that the ratio between the shear and bending stresses is not constant. Consequently, the direction of the principal stresses is not constant and has to be considered for the calculation of the equivalent stresses. Further, the variable amplitude stresses due to torsion and bending have to be matched in an adequate way. For this purpose also the knowlede of the individual cumulative frequency distributions is necessary.

Fig. 4 contains the cumulative frequency distributions for a measuring period of 10.7 minutes. The counting of the level crossings for the given constant mean loads is identical with the counting of the range pairs. Hence follows that there was no

variation of mean loads [2]. As the agitators are not submitted to other unforeseen loads, the measuring time was considered to be large enough in order to obtain representative frequency distributions. Hence, for the fatigue life evaluation for a required service life of 10 years a concervative extrapolation of the loads will be carried out later.

3 EQUIVALENT STRESS

3.1 Determination of the equivalent stress

Fig. 5 summarizes the relations between the maximum bending stresses and the maximum shear stresses. For a preliminary evaluation of the multiaxial stress state the load-time histories are assumed to be constant amplitude loadings with the same frequency.

The short fatigue life to failures of six months with the approximate number of $7 \cdot 10^6$ cycles indicated that the maximum stresses must have been in the order of the endurance limit of the weld.

Since in the design the weld toe and so the very sharp stress concentration is removed, the material state may be evaluated in comparison to the known behaviour of not welded materials. Fatigue testing results under combined torsion and bending show in the high-cycle region no influence of changing principal stress directions as simulated by out-of phase (non-proportional) loading, Fig. 6 and 7a, b [3 to 7]. As the ratio between shear stress amplitudes and bending stress amplitudes in Fig. 6 and 7a, b are much higher than the measured maximum ratio, Fig. 5, the negative influence of the changing principal directions in the shaft-flange connection can be neglected. The calculations due to the hypothesis of effective shear stresses including the influence of normal stresses [3, 4, 8] as well as due to the shear stress intensity hypothesis [5] confirm this statement.

Another parameter which affects the multiaxial fatigue life is the ratio between the frequencies of the torsional and bending load-time histories. The increase of the torsional frequency reduces the fatigue life under multiaxial loading [9, 10], Fig. 7c. In Fig. 7c the multiaxial fatigue strength reducing influence of higher torsional frequency for the ratio of 0.5 between the shear and bending stress amplitudes is more pronounced than the present ratio observed at the shaft of 0.11, Fig. 5. The

calculations [9, 10] carried out under the assumption of constant amplitude loading with the maximum shear and bending amplitudes on the shaft, with the appropriate mean stresses and the higher torsional frequency result in an alternating maximum equivalent stress being about 14 % higher than the bending stress. In the present case this value can be obtained also if the mean stresses and amplitudes are calculated separately due to the von Mises hypothesis [11] and then transformed with a mean stress sensitivity of M = 0.35 for ground welds to a corresponding alternating stress (R = -1).

3.2 Derivation of the equivalent stress spectrum

As the bending stress amplitudes dominate the multiaxial fatigue loading, for the equivalent stress spectrum the shape of the cumulative frequency distribution of bending stresses is used. This spectrum is magnified by the factor of 1.14 as calculated above. This factor includes also the influence of higher frequency of the torsional loading.

This spectrum with $H_{o,\,measured}$ = 315 cycles characterizes only the measuring time of $T_{measured}$ = 10.7 minutes. As the required minimum service life is 10 years, corresponding to T_{total} = 80 000 hours, the spectrum has to be extrapolated to

$$H_{o,\,total} = \frac{T_{total} \cdot H_{o,\,measured}}{T_{measured}} = 1.41 \cdot 10^8 \text{ cycles} \cdot$$

There are several possibilities of extrapolation of the spectrum basing on the measurements. The first one would be to keep the measured maximum value, if higher values are not expected. The second one, which is conservative, is to extrapolate according to the distribution law of the spectrum, for a spectrum length of 10^6, that means from $1.41 \cdot 10^8$ to $1.41 \cdot 10^2$ cyles backwards, and then to keep the maximum, Fig. 8. This kind of extrapolation which was carried out here, assumes that a maximum value which appears once within 10^6 cycles will not be exceeded any more [12]. Another way of extrapolation may be based on the extreme value distribution [2].

The equivalent stress spectrum derived from the load measurements for the critical cross section is originally a nominal stress spectrum. But it is also identical to a local stress spectrum at the critical cross section if notches are removed from this area.

4 FATIGUE LIFE CALCULATION

For the evaluation of the several design alternatives design curves from different codes [13 to 15] and from investigations of LBF were used and derived for a probability of failure of $P_f = 10^{-3}$ and for the failure criterion "first detectable technical crack with a depth of 1 mm". A lower probability of survival was not regarded to be necessary because of recommended periodical inspections. Also stress concentration (K_t), loading-mode and surface treatment dependent slopes (m) of the S-N-curves were taken into account. Because of the protection against corrosion by elastic coatings a respective lowering of fatigue strength is not taken into account.

Damage accumulation calculations were carried out due to a modified linear damage accumulation law [16],

$$D = \sum_{i=1}^{k} \frac{n_i}{N_i} \leq D_{al.} \ ,$$

were the slope of the S-N-curve in the high-cycle region is reduced to m' = 2m-1, as valid for steels and welded joints. Basing on experiences of LBF the allowable damage sum $D_{al.}$ was chosen to be 0.50.

The evaluations are carried out only for the upper shaft-flange connection because the bending stresses are here higher than in the lower connection. Also the stainless steel of the lower shaft-flange connection has the same allowable fatigue properties of the material used in the upper part.

4.1 Evaluation of the original design and first redesign

Fig. 9 shows the individual spectra and design curves on the basis of nominal stresses for the inner and outer diameters of the first redesign, Fig. 3b.

The intersection between the spectrum and dashed design curve on Fig. 9a for the original design explains the failures of the first six stirrers after a short service period even without calculation.

Although in the suggested first redesign the weld is shifted to an area without any other stress concentration and the weld toe is also removed, the damage sum is above the allowable value. In order to reach the required service life it is necessary to push the allowable stresses toward a higher allowable value, for example by a mechanical surface hardening of the welded outer diameter.

But this measure would not be helpful because the failures would start from the inner diameter, Fig. 9b, due to the extremely high local stress concentration. For this reason the proposed first redesign was rejected.

The stress concentration in the transition radius ($K_{tb} \approx 1.8$) between the weld and the flange is not critical, because the allowable stresses of the base material are much higher than the acting stresses.

4.2 Final design

The analysis described above led to the final design, see Fig. 10. The sharp geometrical discontinuity in the inner part of the shaft was removed by turning and a good surface finishing was carried out. The outer diameter was deep rolled after the weld toes were removed and a good surface finishing was achieved. By the rolling operation the hardness of the material was increased by a factor of two. This redesign is accessable to ultrasonics as well as to X-rays and allow therefore a good quality control.

Fig. 11 shows on the basis of local stresses that the calculated damage sums do not exceed the allowable, so that a fatigue life of even more than 10 years can be expected.

5 CONCLUSIONS

It was explained how the random-proportional multiaxial loading and the damage accumulation were taken into account and which steps were performed for the design optimization. Not only the gearbox-sided shaft-flange connection was redesigned but analog to it also the connection on the impeller side. The service experiences won in the past ten years with the redesigned stirrers were successful and have confirmed the design and calculation methodology applied.

6 REFERENCES

[1] Pollard, G.J.:
Hydraulic Loads on Stirrer Shafts and Blades on the F5 Plant
BHRA Fluid Engineering, Bedford/England
BHRA Project No. RP 11 792 (1980), unpublished

[2] Buxbaum, O.:
Betriebsfestigkeit - Sichere und wirtschaftliche Bemessung schwingbruchgefährdeter Bauteile
Verlag Stahleisen mbH, Düsseldorf (1986)

[3] Simbürger, A.:
Festigkeitsverhalten zäher Werkstoffe bei einer mehrachsigen phasenverschobenen Schwingbeanspruchung mit körperfesten und veränderlichen Hauptspannungsrichtungen
Fraunhofer-Institut für Betriebsfestigkeit (LBF), Darmstadt
Bericht Nr. FB-121 (1975)

[4] Grubisic, V.; Simbürger, A.:
Fatigue under Combined Out-of-Phase Multiaxial Stresses
In: International Conference on Fatigue Testing and Design
Society of Environmental Engineers, London (1976), pp. 27.1 - 27.8

[5] Zenner, H.; Richter, I.:
Eine Festigkeitshypothese für die Dauerfestigkeit bei beliebigen Beanspruchungskombinationen
Konstruktion 29 (1977) Nr. 1, S. 11 - 18

[6] Mielke, S.; Troost, A.; El-Magd, E.:
Schwingfestigkeitsverhalten unter zweiachsiger Beanspruchung mit phasenverschobenen schwingenden Normal- und Schubspannungen
Konstruktion 34 (1982) Heft 5, S. 197 - 202

[7] Lempp, W.:
Festigkeitsverhalten von Stählen bei mehrachsiger Dauerschwingbeanspruchung durch Normalspannungen mit überlagerten phasengleichen und phasenverschobenen Schubspannungen
Staatliche Materialprüfanstalt Stuttgart
Techn.-Wiss. Berichte, Heft 77 - 01 (1977)

[8] Grubisic, V.; Sonsino, C.M.:
Rechenprogramme zur Ermittlung der Werkstoffanstrengung bei mehrachsiger Schwingbeanspruchung mit konstanten und veränderlichen Hauptspannungsrichtungen
Fraunhofer-Institut für Betriebsfestigkeit (LBF), Darmstadt
Technische Mitteilungen TM Nr. 79/76 (1976)

[9] Neugebauer, J.:
Zum Schwingfestigkeitsverhalten von Gußwerkstoffen unter mehrachsiger, frequenzverschiedener Beanspruchung
Fraunhofer-Institut für Betriebsfestigkeit (LBF), Darmstadt
Bericht Nr. FB-175 (1986)

[10] Zenner, H.:
Dauerfestigkeit und Spannungszustand
In: VDI-Berichte 661 (1988), S. 151 - 186

[11] Dietmann, H.; Baier, F.:
Spannungszustand und Festigkeitsverhalten (Literaturauswertung)
2. Teil: Schwingende Beanspruchung
Staatliche Materialprüfanstalt Stuttgart
Techn.-Berichte, Heft 71 - 02 (1971)

[12] Haibach, E.; Lipp, W.:
Verwendung eines Einheitskollektives bei Betriebsfestigkeitsversuchen
Fraunhofer-Institut für Betriebsfestigkeit (LBF), Darmstadt
Technische Mitteilungen TM Nr. 15/65 (1965)

[13] DV 804 (Vorausgabe)
Vorschrift für Eisenbahnbrücken und sonstige Ingenieurbauwerke
(VEI) vom 01.01.1979

[14] British Standard BS 5400
Steel, Concrete and Composite Bridges
Part 10, Code of Practice for Fatigue, BSI (1980)

[15] Eurocode Nr. 3
Gemeinsame einheitliche Regeln für Stahlbauten
Kommission der Europäischen Gemeinschaften
Bericht Nr. EUR 8849 DE, EN, FR
Stahlbau-Verlagsgesellschaft mbH, Köln (1984)

[16] Haibach, E.:
Modifizierte lineare Schadensakkumulationshypothese zur Berücksichtigung
des Dauerfestigkeitsabfalls mit fortschreitender Schädigung
Fraunhofer-Institut für Betriebsfestigkeit (LBF), Darmstadt
Technische Mitteilungen TM Nr. 50/70 (1970)

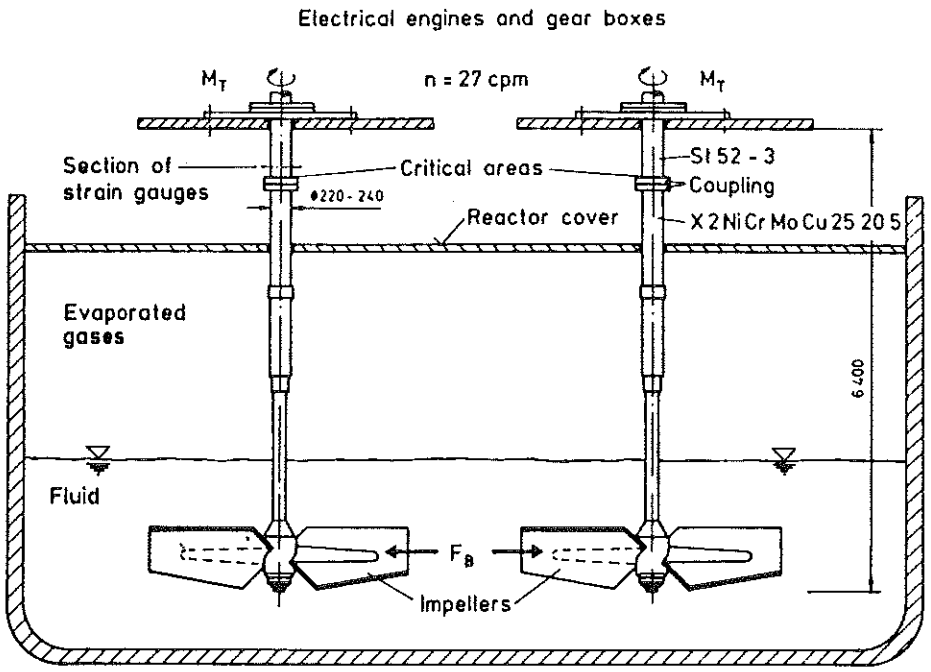

LBF	Stirrers of a Fertilizer Plant	Fig. 1

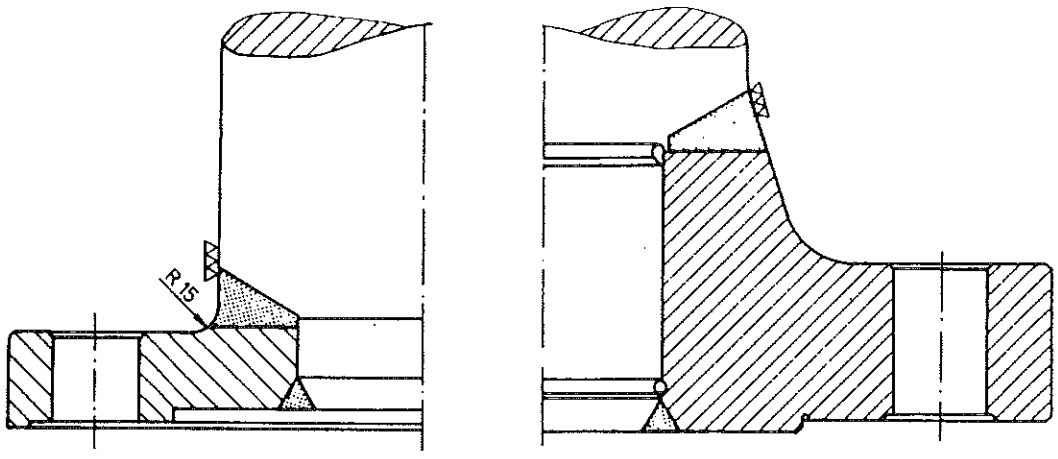

LBF	Welded Flange - Shaft Connections	Fig. 2

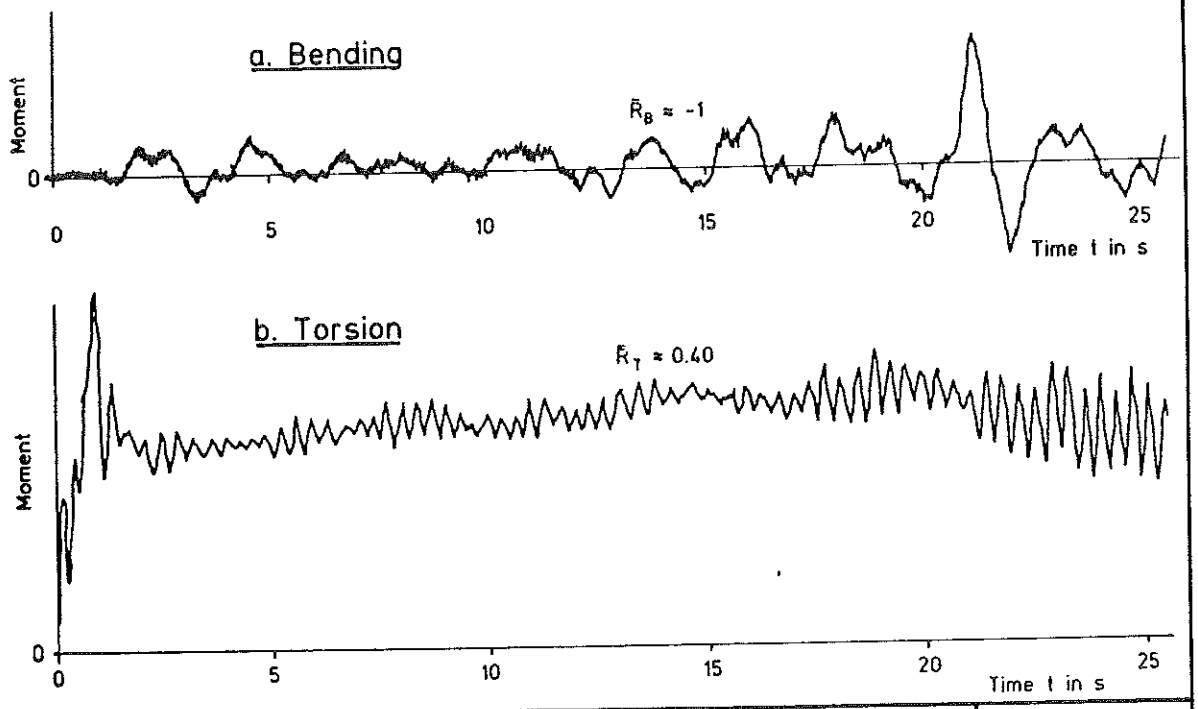

LBF	Multiaxial Random - Load - Time - Histories	Fig. 3

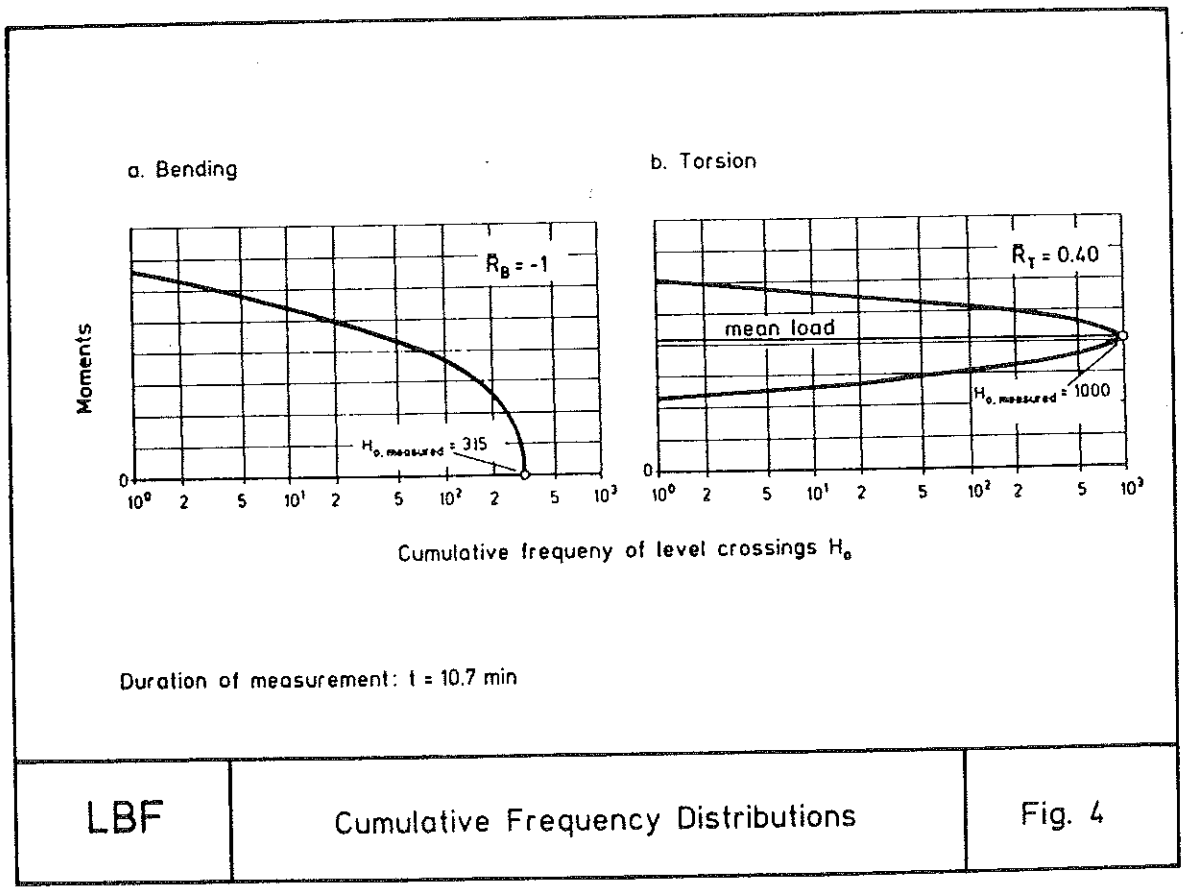

LBF	Cumulative Frequency Distributions	Fig. 4

a. Maximum stress components

Bending:

$\sigma_x = \sigma_{xm} \pm \sigma_{xa} \cdot \sin \omega_x t$

$\sigma_{xm} = 0,\ \sigma_{xa} = \bar{\sigma}_{xa},\ R_\sigma = -1.00$

Torsion:

$\tau_{xy} = \tau_{xym} \pm \tau_{xya} \cdot \sin 6\ \omega_{xy} t$

$\tau_{xym} = 0.30 \cdot \bar{\sigma}_{xa},\ \tau_{xya} = 0.11 \cdot \bar{\sigma}_{xa},\ R_\tau = 0.46$

b. Ratios

Stress components:

$\tau_{xya} / \sigma_{xa} = 0.11,\ \sigma_{xm} / \tau_{xym} = 0$

$\tau_{xym} / \sigma_{xa} = 0.30,\ \omega_{xy} / \omega_x = 6$

Allowable stresses and mean stress sensitivity at $N_f = 2 \cdot 10^6$

$\tau_a (R = -1) / \sigma_a (R = -1) = 0.70$

$M = \dfrac{\sigma_a (R = -1)}{\sigma_a (R = 0)} - 1 = 0.35$

c. Maximum equivalent stress

$\sigma_{eq} = 0 \pm 1.14 \cdot \sigma_{xa} (R = -1)$

LBF	Local Stress Components and Equivalent Stress	Fig. 5

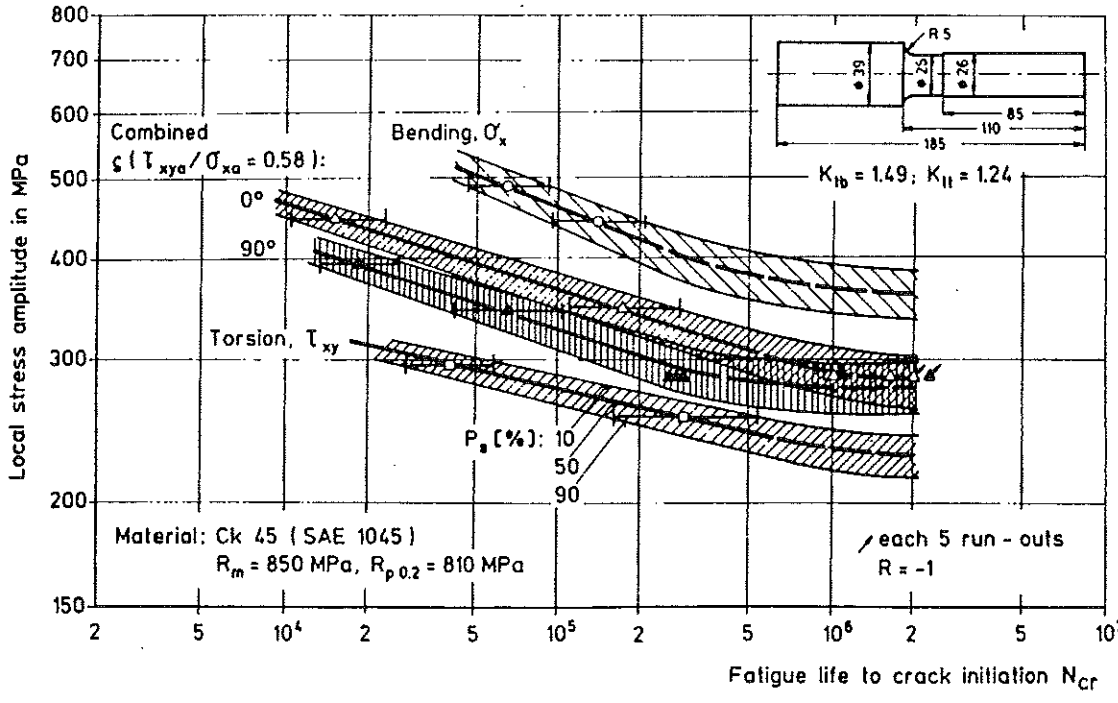

LBF	S - N Curves for Pure and Combined Bending and Torsion	Fig. 6

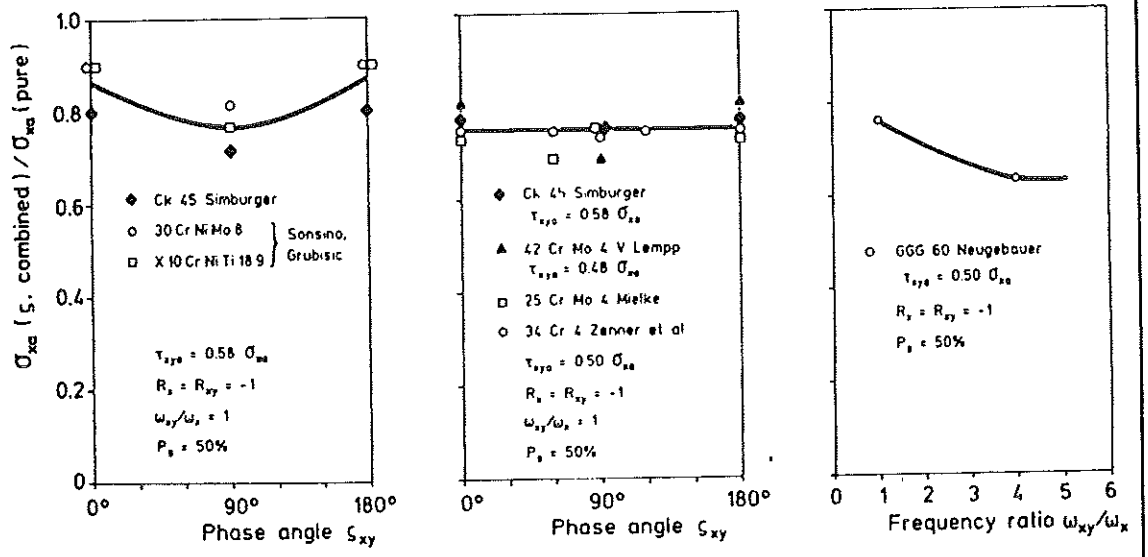

LBF	Influence of Phase Angle and Frequency between Normal and Shear Stresses on Endurable Stress	Fig. 7

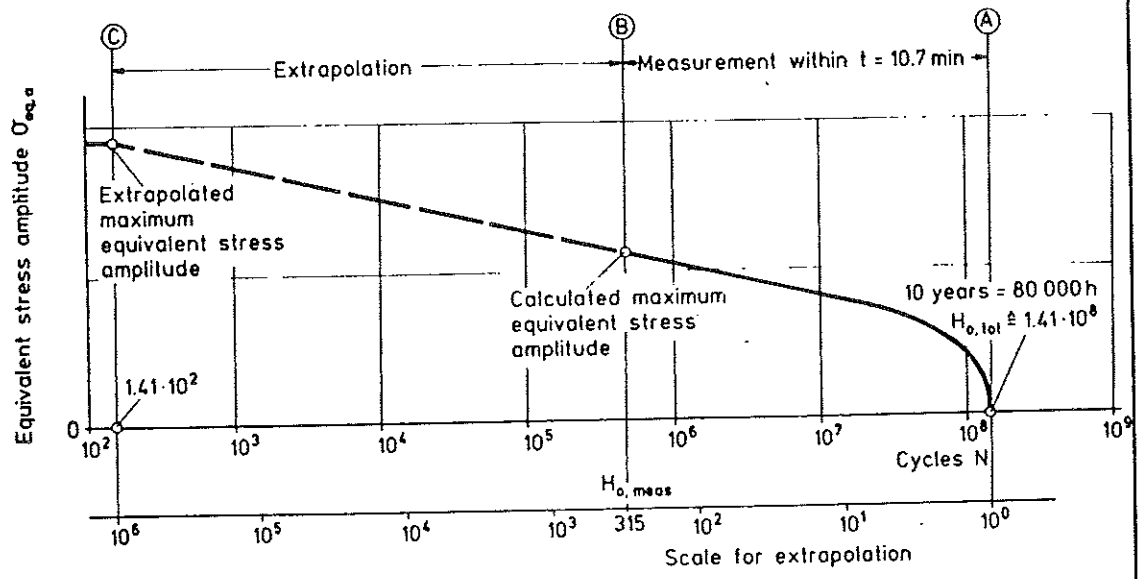

LBF	Derivation of the Equivalent Stress Spectrum for a Service Life of Ten Years	Fig. 8

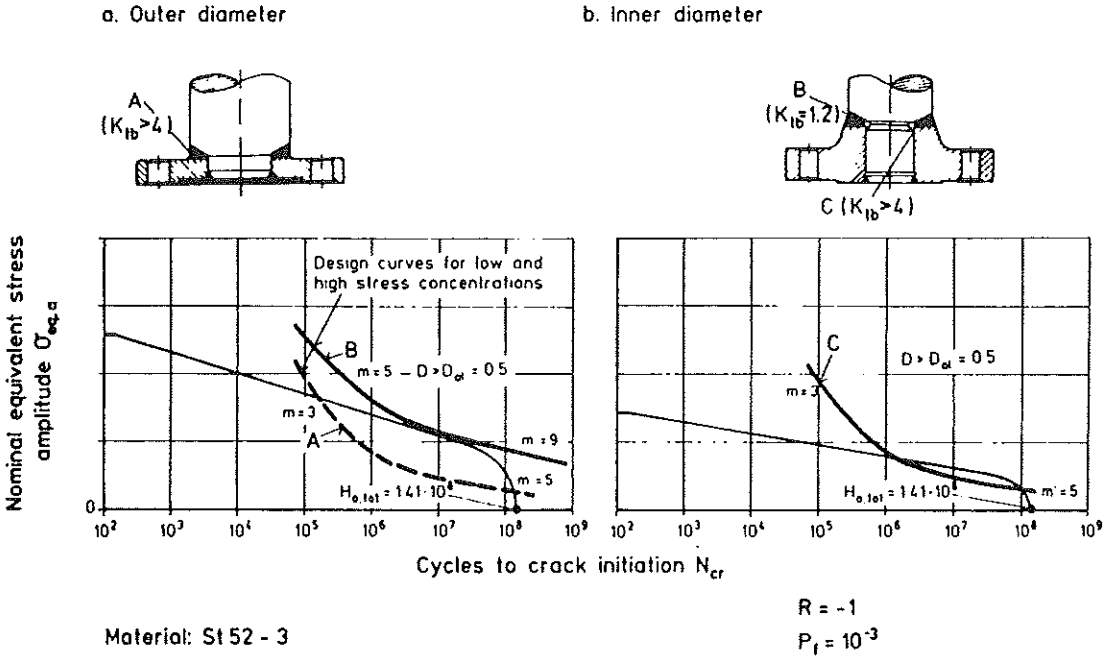

LBF	Fatigue Life Evaluation of the Original Design and First Redesign	Fig. 9

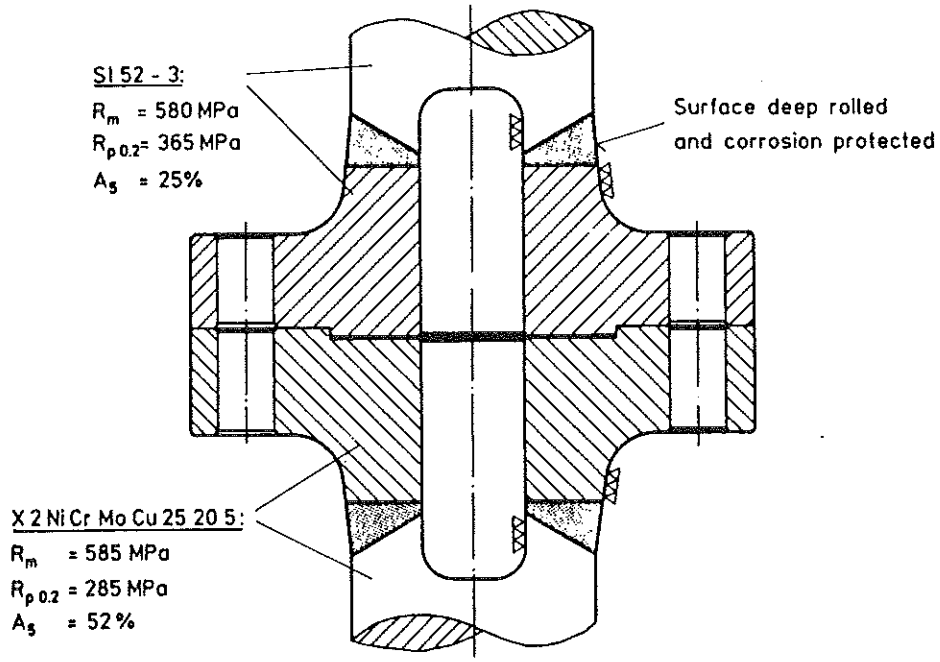

LBF	Final Design of the Welded Coupling Flanges	Fig. 10

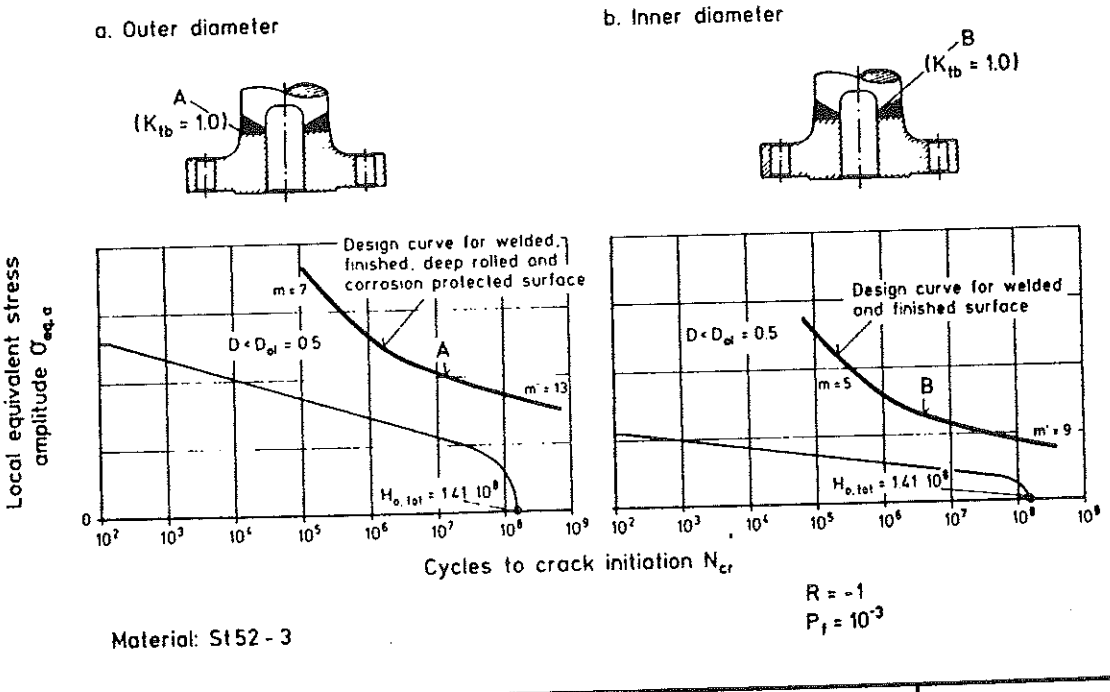

LBF	Fatigue Life Evaluation of the Final Design	Fig. 11